

Development of an integrated four-channel fast avalanche-photodiode detector system with nanosecond time resolution

Zhenjie Li^a, Qiuju Li^a, Jinfan Chang^b, Yichao Ma^c, Peng Liu^a, Zheng Wang^b, Michael Y. Hu^d, Jiyong Zhao^d, E. E. Alp^d, Wei Xu^a, Ye Tao^a, Chaoqun Wu^c, Yangfan Zhou^{a*}

^aBeijing Synchrotron Radiation Facility, Institute of High Energy Physics, Chinese Academy of Sciences, Beijing 100049, China

^bState Key Laboratory of Particle Detection and Electronics, Institute of High Energy Physics, Chinese Academy of Sciences, Beijing 100049, China

^cCollege of electrical & information engineering, Shaanxi University of Science & Technology, Xian, 710021, China

^dAdvanced Photon Source, Argonne National Laboratory, Argonne, IL 60439, USA

^eSchool of Mechanical and Electronic Engineering, Wuhan University of Technology, Wuhan, 430070, China

*Correspondence e-mail: zhouyf@ihep.ac.cn

Abstract: A four-channel nanosecond time-resolved avalanche-photodiode (APD) detector system is developed at Beijing Synchrotron Radiation Facility and the detector system is tested using a single channel for the four-channel system. The detector system consists of three parts: i) four APD sensors, ii) four fast preamplifiers and iii) a time-digital-converter (TDC) readout electronics. The C30703FH silicon APD chips fabricated by Excelitas are used as the sensors of the detectors. It has an effective light-sensitive area of $10 \times 10 \text{ mm}^2$ and an absorption layer thickness of $110 \mu\text{m}$. A fast preamplifier with a gain of 59 dB and bandwidth of 2 GHz is designed to readout of the weak signal from the C30703FH APD. The TDC is realized by a Spartan-6 field-programmable-gate-array (FPGA) with multiphase method in a resolution of 1ns. The arrival time of all scattering events between two start triggers can be recorded by the TDC. The detector has been used for nuclear resonant scattering study at both Advanced Photon Source and also at Beijing Synchrotron Radiation Facility. For the X-ray energy of 14.4 keV, the time resolution, the full width of half maximum (FWHM) of the detector (APD sensor + fast amplifier) is 0.86 ns, and the whole detector system (APD sensors + fast amplifiers + TDC readout electronics) achieves a time resolution of 1.4 ns.

Key words: HEPS-TF, nanosecond time resolution, APD, fast amplifier, TDC

PACS: 07.85.Qe, 29.20.dk, 29.40.Wk

1. Introduction

The silicon avalanche-photodiode (APD) detector system has a number of unique features for X-ray applications such as high counting rate of 10^7 , large dynamic range of 10^9 , sub-nanosecond time resolution, and very low dark counting rate at mHz. It has been widely used in time-resolved experiments, such as nuclear resonant scattering (NRS) with synchrotron radiation [1]. In the NRS experiment [2-4], a strong electronic scattering from the sample occurs promptly on a ps time scale after the incident pulse, while the nuclear resonant scattering is delayed on a 10's of ns time scale by the finite lifetime of the excited state which carry from ns to us. Therefore, one can separate the nuclear delayed events from the electronic scattering ones. The detailed time structure of the nuclear resonant scattering can be measured by a nanosecond time-resolved APD detector system presented here.

The High Energy Photon Source-Test Facility (HEPS-TF) is an R&D project for the planned future High Energy Photon Source (HEPS) in Beijing, China. Development of an APD detector system is a

40 R&D program for the NRS-type of experiments at the new light source. Furthermore, a good APD
41 system can also be used in other experiment, such as the laser pump / X-ray probe experiments, storage
42 ring electron bunch structure and bunch-purity measurements.

43 Time-resolved APD detector systems have been reported before by several research groups [5-10].
44 The APD reported by SPring-8 and KEK are based primarily on silicon sensors fabricated by
45 Hamamatsu Photonics. The APD sensors manufactured by Excelitas are usually adopted by ESRF and
46 APS. Those detector systems have a time resolution between 0.1 ns and 1.7 ns depending on the
47 thickness of chips. However, the time measurement electronics of those traditional detector systems
48 was based on the NIM-modules, which can only record the time of the first delayed nuclear scattering
49 event between two start triggers. Moreover, the NIM-module readout electronics has a low integration
50 and is cumbersome for multiple APD detector system or APD array detector system in the future.

51 In this paper, we have developed a highly integrated APD detector system for NRS experiment. We
52 can realize four-channel TDC readout using Spartan-6 XC6SLX100T chip. The implemented detector
53 system has four APD sensors, four fast preamplifiers, and a time-to-digital convert (TDC) readout
54 electronics. In order to gain sufficient signal-to-noise ratio to detect a single photon, the fast
55 preamplifier with three cascaded amplification stages is designed to readout the weak signal from APD
56 sensor . The TDC readout electronics integrates the NIM-modules functions into one printed circuit
57 board (PCB). The time measurement is based on field programmable gate array (FPGA) TDC, which
58 can record the time of all scattering events between two start triggers. Compared to the current
59 NIM-module, this work mode could record all the photons and improve the experiments efficiency.
60 The detailed design of the developed detector system is discussed in the following sections. The
61 measurement results tested using a single channel for the four-channel system are also presented to
62 demonstrate the capability of the detector system.

63 **2. Design of a nanosecond time-resolved APD detector system**


64 The practical goal of the designed APD detector system is defined to accomplish the ^{57}Fe NRS
65 experiment at a synchrotron radiation beamline. The X-ray energy of ^{57}Fe nuclear resonance is 14.4
66 keV, while the lifetime of this radiation is 141 ns. The targeted efficiency of the APD detector system
67 is larger than 10 % at 14.4 keV, and the count rate should be larger than 10^6 photons/s. Since the
68 detector must recover quickly to record a nuclear scattering event a few 10's ns later, the output pulse
69 width at base of the preamplifier should be less than 20ns. In some experiments the nuclear resonant
70 scattering event may be as low as 0.1 Hz, so the dark count rate of our detector system is designed to be
71 as low as 0.01 Hz. In addition, the time resolution of < 2 ns is also needed to capture the arrival time of
72 scattering events accurately. The design specification is summarized in Table 1. The simultaneous
73 requirement of high efficiency, high counting rate, fast recovery time, and very low dark counting rate
74 is very challenging in the detector system design.

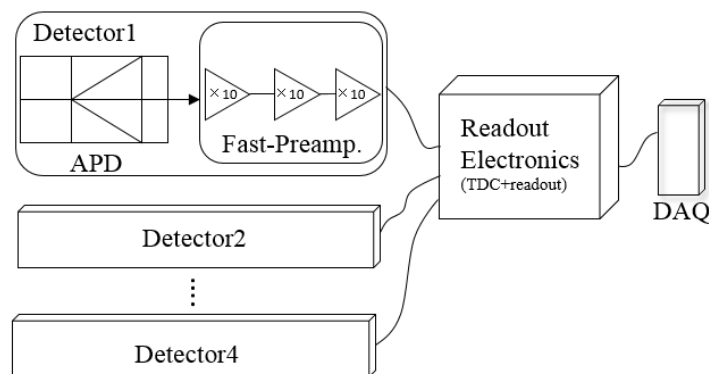
75 Fig.1 shows the implemented four-channel APD detector system diagram. Each detector consists of
76 an APD sensor and a fast preamplifier. A TDC readout electronics handles four readout channels. Each
77 readout channel can accomplish the functions of signal inversion, discrimination and TDC. The time
78 data, obtained by the TDC readout electronics, is transmitted to a data acquisition (DAQ) unit via a
79 single optical fiber.

80

81

Table1 Design specification of the implemented APD detector system

Parameter	Requirement
Efficiency	> 10 %
Count rate	> 1 MHz
Output pulse width of the pre-amplifier	< 
Dark counting rate	< 0.01 Hz
Time resolution	< 2 ns



83

84

Fig. 1. Structure of the detector system

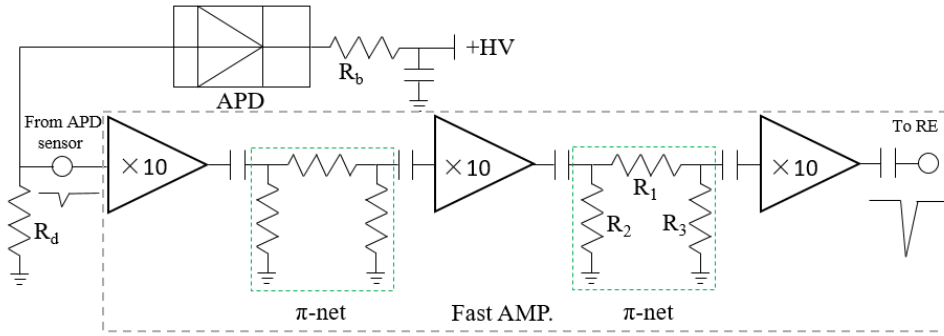
85 2.1 Si-APD sensor

86 The APD sensor used in this detector system is C30703FH which is fabricated by Excelitas
 87 Technologies. The sensor is designed on a 120 μm thick silicon wafer with reach-through structure [11].
 88 The avalanche amplification region located on the back of the device is very narrow, so the device
 89 presents an absorption layer thickness about 110 μm . This absorption thickness makes the sensor
 90 calculated efficiency 25 % at the energy of 14.4 keV. The APD gain is about 50-100 when the high
 91 voltage is set from 300V-400V. The sensitive area of this sensor is $10 \times 10 \text{ mm}^2$, which provides a
 92 sufficient solid angle for inelastically scattered X-ray detection.

93 2.2 Fast preamplifier

94 The current signals from the APD are processed by a high bandwidth 2 GHz, high gain 59 dB
 95 preamplifier. The schematic diagram of the fast preamplifier is shown in Fig. 2. The preamplifier
 96 consists of three Mini circuits Mar6+ commercial amplifier chips and two π -type resistant networks.
 97 These amplifier chips are cascaded in three stages to get a gain of about 60 dB. To increase the stability
 98 of the preamplifier, the π -type resistant networks are added between two amplifier chips, and they are
 99 designed with individual components.

100 The input impedance of the π -type resistant networks should be matched with the output impedance
 101 of the signal, and the output impedance of the π -type resistant networks should be matched with the
 102 load.



103

104 Fig. 2. Schematic of the fast preamplifier. R_b limits the bias current and R_d is closed to the bias circuit. The pulse of the fast
 105 signal from APD capacitive coupled to the first stage amplifier

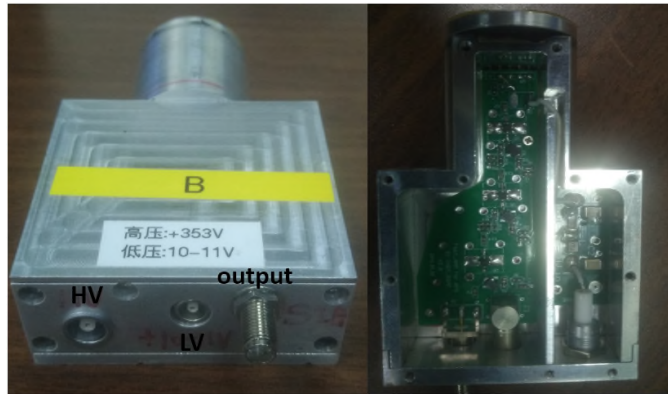
106 The calculation of networks is shown in the formula below

107

$$Z_m = R_2 P(R_1 + R_3 P 50\Omega) = 50\Omega$$

108 Here, the values of the resistances are $R_1 = 10 \Omega$, $R_2 = R_3 = 300 \Omega$. The attenuation for one π -type
 109 networks is 0.28 dB. Since the gain of the commercial amplifier chip is 20 dB, the preamplifier has a
 110 gain of 59 dB.

111 The fast preamplifier is first designed and fabricated on a printed circuit board. The preamplifier
 112 board is sitting in an aluminium box to shield the environmental electromagnetic radiation.
 113 Furthermore, the high voltage circuit of the APD sensor is isolated from the fast preamplifier by an
 114 aluminium wall in the box. Therefore, the high voltage circuit will not induce noise to the fast
 115 preamplifier. Through the above measures, a stable preamplifier with high bandwidth and high gain is
 116 implemented. The fast preamplifier with APD sensor is shown in Fig.3.



117

118 Fig.3 The real picture of the preamplifier sitting in the box with high voltage and signal separated

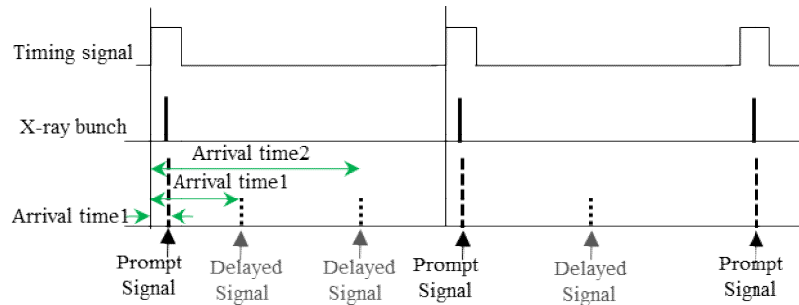
119 2.3 TDC readout electronics

120 Compared to the NIM-module TDC, the FPGA TDC we designed is much more integrated and it can
 121 used in multi-element or array APD detector system in the future. Fig. 4 shows the logic diagram of the
 122 time measurement for NRS experiment. The timing signal is the RF signal from the storage ring and it
 123 works as the start signal of the TDC. A prompt and a delayed signal work as the stop signal of the TDC.
 124 The time, defined as the time difference between the start signal and the stop signal, is measured by the

125 TDC. In our system, the TDC readout electronics can measure one or more scattering events after the
 126 start signal, which is an advantage over the current NIM-module used in NRS.

127 Fig. 5 shows the structure of one channel TDC. Signals from the fast preamplifier are modulated by
 128 the stage A1, which magnifies the signal several times and changes the polarity of the signal from
 129 negative to positive, so that the signal can be detected by the discriminator (TH). A digital-to-analogue
 130 converter (DAC) is added to adjust the discrimination threshold. Then the time between the start signal
 131 and the stop signal is measured by the FPGA TDC.

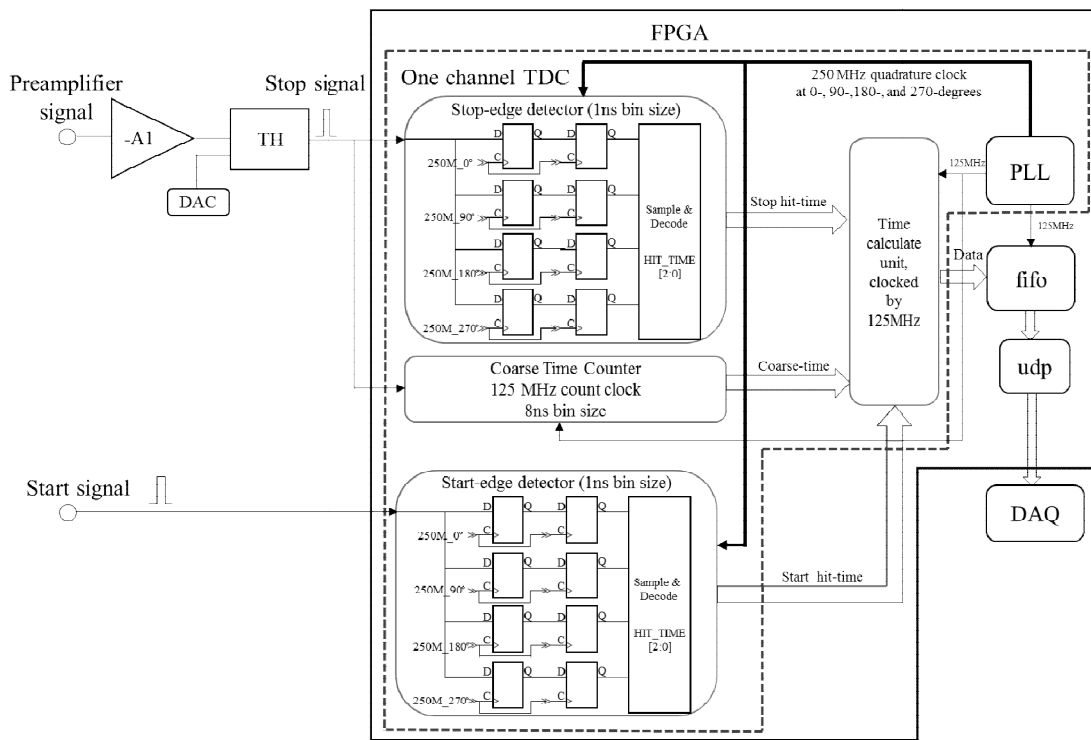
132



133

134

Fig. 4. Logic diagram of the time measurement for NRS experiment



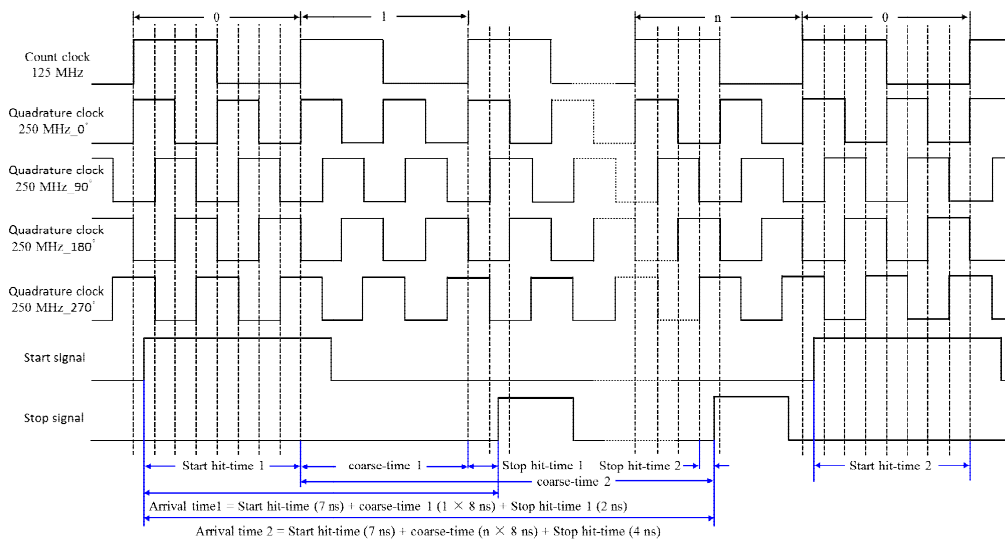
135

136

Fig. 5. Structure for one channel of the TDC readout electronics

137 The TDC uses a multi-phase technology and is realized in an FPGA Spartan-6 XC6SLX100T
 138 chip [12]. It consists of a stop-edge detector, a shared start-edge detector, a coarse-time counter, a
 139 time-calculation unit, and a shared phase lock loop (PLL). The PLL creates a 250 MHz quadrature
 140 clock with 0-, 90-, 180-, and 270-degree shifts for the stop edge detector and the shared start-edge
 141 detector. The PLL also generates a 125 MHz clock for the coarse-time counter. Each phase of the
 142 quadrature clock operates at 250 MHz, essentially creating a clock that operates at 1 GHz. The

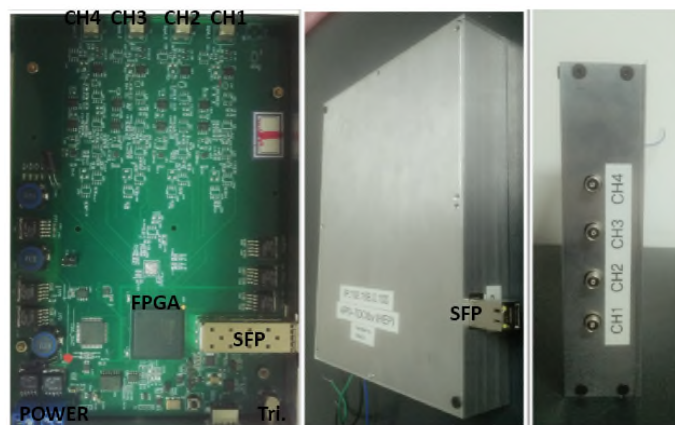
143 stop-edge detector detects the rising edge of the stop signal and records the stop hit-time in every
 144 period of 8 ns. The quadrature clock makes the equivalent to of a 1 GHz clock, and the resolution size
 145 of the stop-edge detector is 1ns. The start-edge detector records the start hit-time using the same
 146 working principle as the stop-edge detector. The coarse-time counter counts at a count clock of 125
 147 MHz, with a period of 8 ns. The time calculation unit calculates the time by combining the start
 148 hit-time, stop hit-time and the coarse-time. The timing diagram of the TDC is simply illustrated in Fig.
 149 6, and the time = start hit-time + coarse-time + stop hit-time, with a fixed time-stamp resolution of 1 ns
 150 per bin. The dead time of the TDC for each event is about 30ns for the spending of the time calculation.
 151 Then, the data of the arrival time are output through the first-in first-out (FIFO) buffer and the user
 152 datagram protocol (UDP) to the data acquisition (DAQ) system.



153
 154

Fig. 6. Timing diagram of the TDC

155 Using the Spartan-6 XC6SLX100T chip, in order to meet the sequential relationship, four channel
 156 TDC could be designed in the limiting case. The TDC's scalable time range is from 1ns to 4096ns with
 157 1ns bin. The TDC readout electronics is shown in Fig.7. The PCB size is



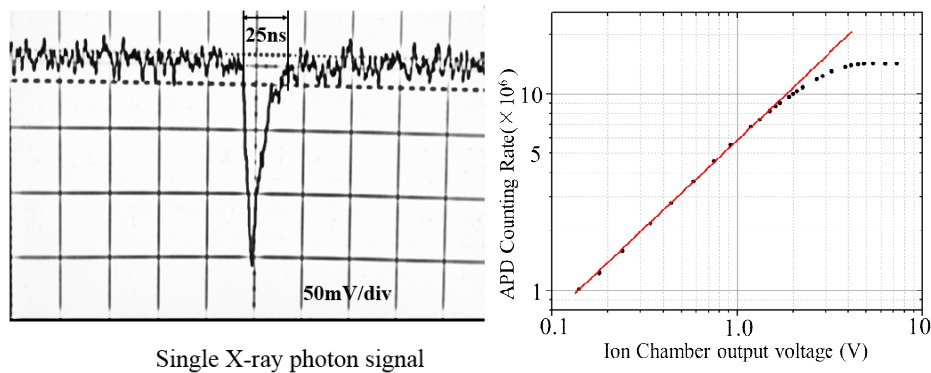
158
 159

Fig.7 The picture of real TDC PCB board.

160 **3. Performance**

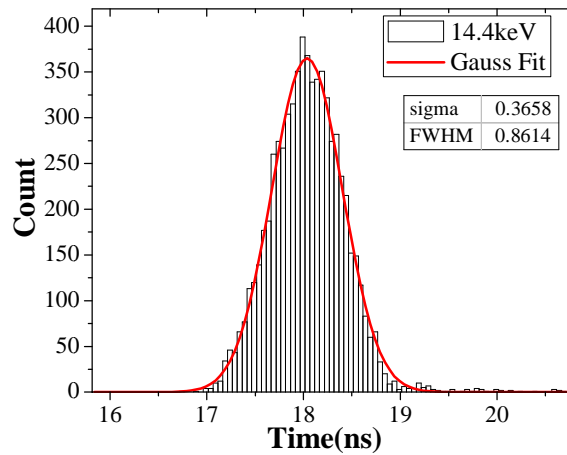
161 **3.1 APD detector performance**

162 The APD sensor and the fast preamplifier are housed in an aluminium box and tested as an X-ray
 163 detector at 1W2B experiment station of Beijing Synchrotron Radiation Facility (BSRF). The output
 164 pulse from the detector is shown in Fig. 8 (a), the output signal height is about 150mV when the photon
 165 energy is 14.4keV, and the pulse width at base is about 25 ns. In order to estimate the count rate, the
 166 APD detector linearity at high count rate was investigated. The measured counting rate versus the input
 167 X-ray intensity monitored by the ion chamber and represented using ion chamber output voltage is
 168 shown in Fig. 8 (b). From the result, one can see that the detector has a good linearity below the count
 169 rate of 8-10 MHz. The dark counting mainly comes from the cosmic ray, by setting the threshold half
 170 of the pulse height (75mV), the dark counting rate is less than 0.01Hz.



172 Fig. 8. (a) Single X-ray photon signal pulse, (b) Counting rate vs Ion Chamber output voltage

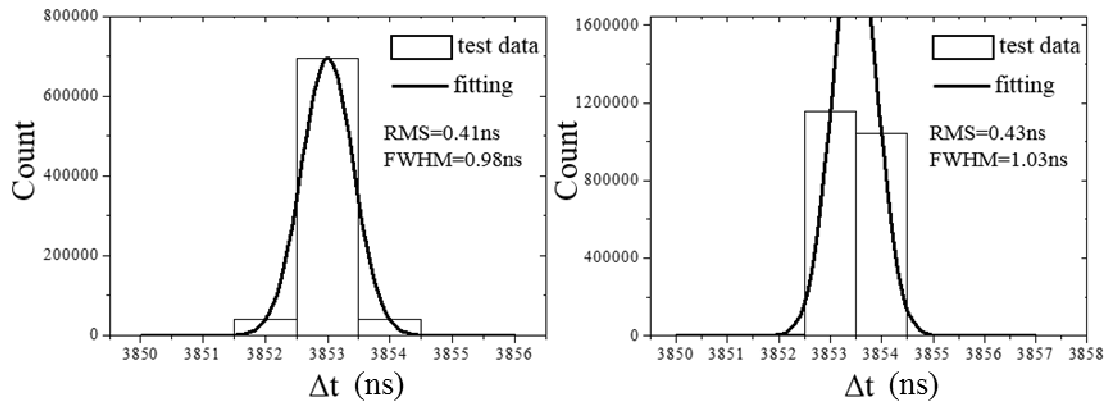
173 The time resolution of the designed APD detector is also investigated by measuring the arrival time
 174 of the X-ray photon after the locked RF signal from the accelerator storage ring. The FWHM time
 175 resolution of the detector is 860 ps with the threshold of 75mV (@14.4 keV), as shown in Fig. 9.



177 Fig. 9. Time resolution of the APD detector

178 3.2 TDC readout electronics performance

179 In the TDC readout electronics test, the threshold is set at half amplitude of the inverting buffer
 180 output swing. The resolution of TDC readout electronics is tested by using a high precision signal
 181 generator. Fig. 10 shows the time resolution of TDC in different situations: the integer input delta time
 182 and the input delta time with a decimal part of 0.5. The results indicate that the FWHM resolution is
 183 about 1ns, even in the worst input delta time case.

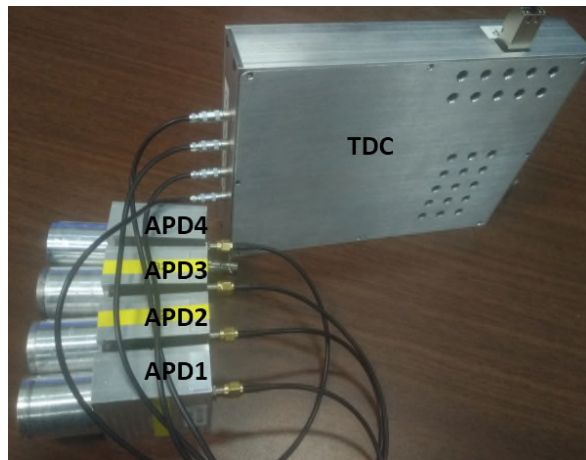


184

185 Fig. 10. (a) Time resolution of TDC electronics when the input delta time is 3853 ns; (b) time resolution of TDC electronics
 186 when the input delta time is 3853.5 ns

187 **3.3 Time resolution of the detector system**

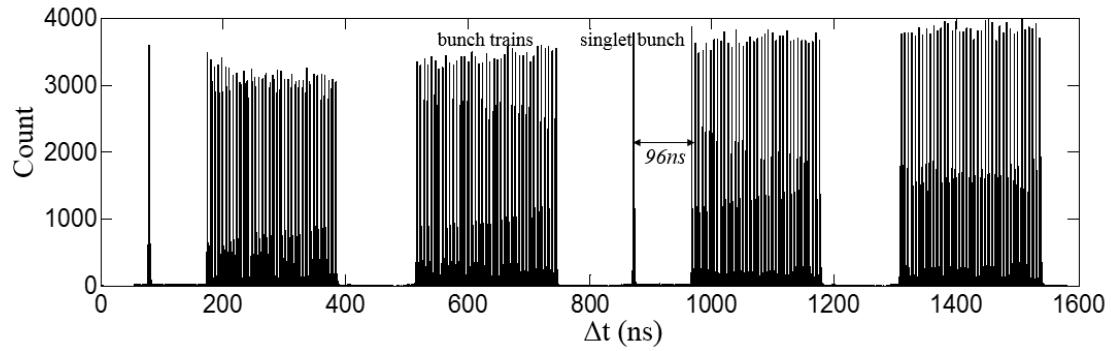
188 This APD detector system is further tested at 1W2B experiment station of BSRF. In the test, the RF
 189 signal from the accelerator storage ring serves as a start signal of the TDC and the X-ray photon signals
 190 are the stop triggers for the TDC. Fig.11 shows the real connection of the system, the APD detectors
 191 with preamplifiers were connected to the TDC. In the test results, we use one of the four channels to
 192 verify the time resolution of the system.



193

194 Fig.11 The APD detector system both with APD and TDC

195 Fig. 12 shows the measured time structure of the electron beam bunch of BSRF by using the
 196 developed APD detector system. The maximum count rate for each channel is 10MHz, which is limited
 197 by the APD signal pulse width, the synchrotron bunch mode and the data transfer. The electron beam
 198 bunch structure has a hybrid fill pattern in which a specific single bunch is filled with sufficient interval
 199 from other bunches. Fig. 13 shows the measured time resolution of the detector system at 14.4 keV and
 200 the overall time resolution FWHM is 1.4 ns.

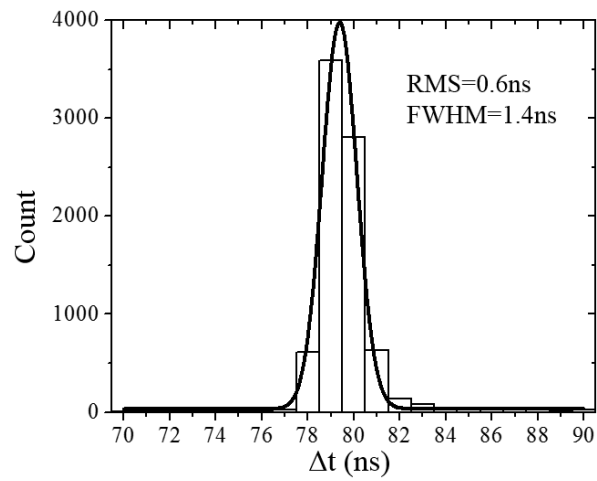


201

202

Fig. 12. Time structure of the beam bunch at BSRF: hybrid bunch structure with a singlet bunch. The interval between the
 203 singlet bunch and the bunch trains is about 96 ns

204



205

206

Fig. 13. Time resolution of the APD detector system

207

208

209

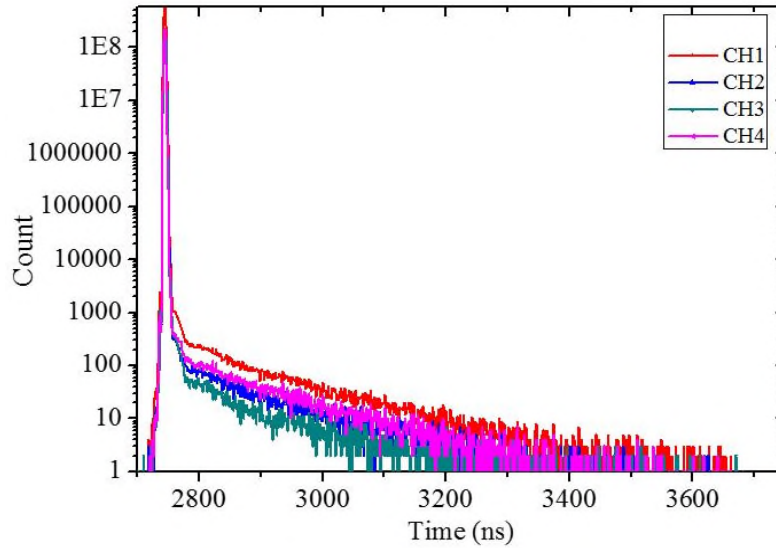
210

211

212

213

The designed detector system was employed for the nuclear resonant scattering experiments of samples at 3-ID beamline, Advanced Photon Source. In this experiment, the synchrotron Mössbauer spectra in time domain were collected with acceptable signal-to-noise ratio. Fig.14 shows the results of the experiment data. We use four APD detectors to detect the nuclear resonant scattered photons and the four channels could collect the photon time data at the same time, showing the same results in agreement with conventional Mössbauer spectroscopy. Therefore, we can improve the experiments efficiency if we use more APD detectors in the future.



214

215 Fig. ⁵⁷Fe nuclear scattering experimental results with the designed detector system (Data taken at 3-ID Beamline of the
 216 Advanced Photon Source, USA).

217 **4. Conclusions**

218 We have developed an integrated four-channel nanosecond time-resolved APD detector system
 219 based on single element APD sensor. It can be used for NRS experiments in HEPS-TF project. In the
 220 future, the multi-element or array APD detector system will be designed using this four-channel TDC
 221 readout electronics. The effective light-sensitive area of $10 \times 10 \text{ mm}^2$ and the efficiency of 25% @ 14.4
 222 keV X-ray photons are achieved by utilizing the C30703FH silicon APD chips as the detector sensor.
 223 The fast preamplifier is designed on the discrete components with gain of 59 dB and bandwidth of 2
 224 GHz. The TDC, with a resolution of 1ns, is realized by FPGA with multiphase method, which can
 225 record the time of all scattering events between two start signals. However, the existing NIM module
 226 system could only record one photon time between two start signals. The measured results indicate that
 227 the APD detector system time resolution is 1.4 ns. This novel APD detector system can be used for the
 228 nuclear resonant scattering technique, as well as pump/probe time-resolved experiment in the current
 229 synchrotron radiation facilities. It will also greatly promote the development of the NRS program in the
 230 future High Energy Photon Source in China.

231

232 **Acknowledgements**

233 This work is supported by the National Natural Science Foundation of China (Grant No. 11605227),
 234 the key technologies R & D program of Hubei Province of China (No. 2015BCE076), the High Energy
 235 Photon Source-Test Facility Project, and the State Key Laboratory of Particle Detection and
 236 Electronics. Authors thank Prof. Jun-Hu Wang and Prof. A. I. Rykov of DIPC-CAS for providing the
 237 samples to be tested. This research used resources of the BSRF and this research also used resources of
 238 the APS, a US DOE Office of Science User Facility operated for the DOE Office of Science by
 239 Argonne National Laboratory under Contract No. DE-AC02-06CH11357.

240

241

242

243 **References**

- 244 [1] A. Q. R. Baron et al. *J. Synchrotron Rad.* 13 (2006) 131.
- 245 [2] G.V. Smirnov. *Hyperfine Interactions.* 97/98 (1996) 551.
- 246 [3] Makoto SETO. *J. Phys. Soc. Jpn.* 82 (2013) 021016-1.
- 247 [4] W. Sturhahn, et al, *Phys. Rev. Lett.* 74 (1995) 3832.
- 248 [5] Shunji Kishimoto. *Rev. Sci. Instrum.* 66 (1995) 603.
- 249 [6] Shunji Kishimoto. *J. Synchrotron Rad.* 5 (1998) 275.
- 250 [7] A. Q. R. Baron. *Nucl. Instrum. Methods Phys. Res. A* 343 (1994) 517.
- 251 [8] A. Q. R. Baron et al. *Nucl. Instrum. Methods Phys. Res. A* 400 (1997) 124.
- 252 [9] A. Q. R. Baron. *Hyperfine Interactions.* 125 (2000) 29.
- 253 [10] T. Toellner, et al, *Nucl. Instrum. Methods A* 350 (1994) 595.
- 254 [11] A. Q. R. Baron. *Nucl. Instrum. Methods Phys. Res. A* 352 (1995) 665.
- 255 [12] Fries M D et al. *Nuclear Science Symposium Conference Record, IEEE.* 1 (2002) 580.